

G-protein alpha and beta–gamma subunits interact with conformationally distinct signaling states of rhodopsin

Maureen A. Downs^a, Rieko Arimoto^{c,1}, Garland R. Marshall^c, Oleg G. Kisselev^{a,b,*}

^a Department of Ophthalmology, Saint Louis University School of Medicine, St. Louis, MO 63104, USA

^b Department of Biochemistry and Molecular Biology, Saint Louis University School of Medicine, St. Louis, MO 63104, USA

^c Department of Biochemistry and Molecular Biophysics, Washington University School of Medicine, St. Louis, MO 63110, USA

Received 9 June 2006; received in revised form 13 July 2006

Abstract

Light activated rhodopsin interacts with domains on all three subunits of transducin. Two of these domains, the C-terminal regions of the alpha and gamma subunits mimic the ability of transducin to stabilize the active conformation of rhodopsin, metarhodopsin II, but display different roles in transducin activation process. Whether the interactions are with the same or different complimentary sites on Meta II is unknown. We have used chemo-selective thioalkylation of rhodopsin and UV/visible spectroscopy to show that interactions with transducin C-terminal domains can be selectively disrupted. These data provide evidence that formal structural determinants on Meta II for these domains of transducin are different. In a set of complimentary experiments we examined the reactivity of Meta II species produced in the presence of the Gt α and Gt γ subunit peptides to hydroxylamine. Analysis of the rates of Meta II decay confirms that the conformational states of Meta II when bound to Gt α and Gt $\beta\gamma$ represent distinct signaling states of rhodopsin.

© 2006 Elsevier Ltd. All rights reserved.

Keywords: Rhodopsin; Transducin; Alpha subunit; Beta–gamma subunit complex; Phototransduction; Signaling

1. Introduction

A prototypical seven transmembrane (7TM) domain receptor, rhodopsin, interacts with a heterotrimeric G-protein, transducin, to initiate a visual signaling cascade in response to light activation of rod photoreceptors (Hargrave, 2001; Kisselev, 2005). Despite available X-ray structures of rhodopsin and transducin, and extensive mapping of the rhodopsin–transducin interface, the exact mechanism of rhodopsin-catalyzed nucleotide exchange on transducin remains poorly understood. On rhodopsin, the site of interactions with the G-protein is comprised of cytoplasmic loops C2, C3, and a short helix in C4 (H8) (Okada, Ernst, Palczewski, & Hofmann, 2001; Park, Filipek, Wells, & Palczewski, 2004; Ridge, Abdulaev, Sousa, & Palczewski, 2003; Sakmar, Menon, Marin, &

Awad, 2002). The footprint from the light-activated rhodopsin on transducin is fairly large, and includes several regions on the Gt α -, Gt β -, and Gt γ -subunits. The C-terminal binding domains of the Gt α - and Gt γ -subunits are the major receptor recognition regions (Gautam, Downes, Yan, & Kisselev, 1998; Hamm, 2001). They are of special interest, because of the ability to mimic holo-transducin in stabilizing the active photointermediate of rhodopsin, metarhodopsin II, Meta II, or R* (Hamm et al., 1988; Kisselev, Ermolaeva, & Gautam, 1994). Both domains, Gt α (340–350), Gt α CT and Gt γ (60–71)farnesyl, Gt γ CT have been implicated in a two-step sequential fit hypothesis, which argues for a temporal separation in interactions between Gt α and Gt $\beta\gamma$ with R* (Herrmann et al., 2004; Kisselev, Meyer, Heck, Ernst, & Hofmann, 1999a). It has been specifically suggested that Gt γ CT makes initial contacts with R*, while Gt α CT is involved at the second step in R*-catalyzed nucleotide exchange. Despite this information, the dynamics of Gt α CT and Gt γ CT in the R*–Gt complex is sketchy. The question of whether light activated rhodopsin

* Corresponding author. Fax: +1 314 771 0596.

E-mail address: kisselev@slu.edu (O.G. Kisselev).

¹ Present address: Vertex Pharmaceuticals, Cambridge, MA, USA.

presents two independent sites for interactions with these domains of the Gt α - and Gt γ -subunits remains unresolved. It is also unknown whether different conformations of Meta II are involved during binding to Gt α and Gt $\beta\gamma$ in the sequential fit hypothesis.

In order to probe the cytoplasmic surface of rhodopsin for the presence of two sites complementary to Gt α CT and Gt γ CT, we have used chemo-selective modifications of cysteine residues at positions 140 and 316 with *N*-ethyl-maleimide (NEM) and iodoacetamidosalicylate (IAS) and their derivatives, and measured how modified R* interacts with holo-Gt in biochemical binding experiments. Both cysteines are conveniently situated in the general vicinity of the known sites for Gt on the rhodopsin cytoplasmic surface. Chemical modifications of these residues introduce potential steric hindrances at R*-Gt interface and provide an opportunity to selectively block interactions with Gt α and Gt $\beta\gamma$ binding domains. Analysis of interactions between individual domains of R* and Gt is difficult because of strong allosteric effects in the R*-Gt complex. To circumvent these allosteric complications, we probe modified rhodopsin with synthetic peptides specific to Gt α CT and Gt γ CT by UV/visible spectroscopy. Finally, we directly probe Meta II conformations produced in the presence of either Gt α CT or Gt γ CT by hydroxylamine, a rhodopsin conformation-sensitive reducing agent. The Schiff base of the retinal is extremely sensitive to the attack by hydroxylamine when rhodopsin is in the Meta II state. This increased reactivity is the direct result of the light-triggered conformational changes in rhodopsin, and the opening of the transmembrane bundle. We use UV/visible and single wavelength rapid scanning spectroscopy to monitor hydroxylamine-induced Meta II decay. Our results provide support to the sequential fit hypothesis and argue that after light activation of rhodopsin, Gt α and Gt $\beta\gamma$ interact with conformationally distinct signaling states of R*.

2. Materials and methods

2.1. Rhodopsin and Gt isolation

Dark adapted frozen bovine retinas are obtained from W.L. Lawson, Co. (NE). Rod outer segments (ROS) are prepared by the method of Papermaster and Dreyer (Papermaster & Dreyer, 1974). Urea-washed ROS membranes (UM) are prepared using the procedure adapted from Yamazaki et al. (Yamazaki, Bartucca, Ting, & Bitensky, 1982), and Willardson et al. (Willardson, Pou, Yoshida, & Bitensky, 1993), essentially as we described earlier (Kisselev, Pronin, & Gautam, 1999b). Rhodopsin concentration is measured as ΔA_{498} before and after bleaching in the presence of 20 mM hydroxylamine, based on the molar extinction coefficient at 498 nm of $42,700 \text{ M}^{-1} \text{ cm}^{-1}$ (Hong & Hubbell, 1972). Gt was purified by GTP elution from isotonic washed ROS disks, and Gt α and Gt $\beta\gamma$ were separated by AKTA FPLC on Blue-Sepharose Cl-6B. The purity of rhodopsin and transducin were also assessed by SDS-PAGE and protein staining with silver (Wray, Boulikas, Wray, & Hancock, 1981).

2.2. Selective double labeling of rhodopsin

Modifications at cysteine 140 with *N*-ethyl-maleimide (NEM) and at cysteine 316 by iodoacetamidosalicylate (IAS) was performed using a procedure adapted from De Grip (De Grip, Bonting, & Daemen, 1975) and Sale (Sale,

Towner, & Akhtar, 1977). Dark-adapted rhodopsin in urea treated ROS membranes ($1.35 \times 10^{-4} \text{ M}$ rhodopsin) were suspended in 0.2 M potassium phosphate buffer, pH 7.0. IAS was dissolved in a small volume of ethanol. The reaction was started by adding a 20-fold molar excess of IAS in 0.2 M potassium phosphate buffer, pH 7.0. After incubation for 18 h at 20 °C in the dark, samples were diluted by 16 reaction volumes of an ice-cold 0.2 M potassium phosphate buffer, pH 7.0, and centrifuged (4 °C, 16,000g, 30 min). Pellets were washed with the same buffer followed by centrifugation (4 °C, 16,000g, 30 min). ROS were then resuspended again at $1.35 \times 10^{-4} \text{ M}$ rhodopsin and further incubated with a 100-fold molar excess of [^3H]NEM (*N*-[ethyl-1,2- ^3H]maleimide, specific radioactivity $1.7 \times 10^7 \text{ dpm}/\mu\text{M}$) for 9 h at 20 °C. Samples were finally washed twice with an excess of ice cold 0.2 M potassium phosphate buffer, pH 7.0, and either processed immediately or frozen at -80 °C. For a non-selective modification of both cysteine 140 and cysteine 316 by [^3H]NEM, the same procedure was followed except that no IAS was added before the first 18 h incubation. The amount of rhodopsin in samples was determined both spectroscopically and using Bio-Rad Protein Assay. To confirm the site of thioalkylation reported earlier (De Grip et al., 1975; Findlay et al., 1984), aliquots of samples were treated with the endoprotease V8 (Sigma) in 50 mM ammonium bicarbonate buffer, pH 7.5, for 30 min at 37 °C (0.5 U/9 nmol of rhodopsin) to produce rhodopsin fragments Rh(1–239), Rh(240–341) and a small C-terminal fragment Rh(342–348) (Sale et al., 1977). Samples were subjected to Laemmli SDS-PAGE under non-denaturing conditions. Gels were stained with Coomassie blue R-250 and cut in 2 mm slices. The slices were placed in counting vials and incubated for 3 h at 50 °C in the presence of gel solubilizer, Solvable (NEN). After addition of the scintillation fluid, the vials were counted in a Beckman scintillation counter (model LS 1801). For UV/visible spectroscopic measurements, rhodopsin was prepared as above with non-radioactive NEM and IAS. As expected, only two cysteines were modified by NEM, Cys 140 found in the proteolytic fragment Rh(1–239), and Cys 316 found in fragment Rh(240–341), while pre-treatment with IAS selectively protected Cys 316. In preparation of spin-labeling experiments, three sulfhydryl specific derivatives of 2,2,5,5-tetramethylpyrrolidine-*N*-oxyl (PROXYL) were used, 3-iodoacetamido (IA)-PROXYL, 3-methyl-methanethiosulfonate (MTS)-PROXYL, and 3-maleimido-PROXYL (TRC Inc.).

2.3. Gt binding to ROS membranes

Various amounts of the Gt $\beta\gamma$ (0–10 μg) were reconstituted with 10 μg of Gt α and 30 μg of urea-washed ROS membranes, UM, in 100 μl of buffer ROS-ISO (10 mM Tris, pH 7.4, 100 mM NaCl, 5 mM MgCl₂, 1 mM DTT, and 0.1 mM PMSF) on ice. The reaction was initiated by exposure to light. UM were centrifuged at 109,000g, 4 °C for 10 min in a TLA-100.3 rotor on a Beckman TL-100 Ultracentrifuge. The pellet was washed twice with buffer ROS-ISO. UM with Gt bound was resuspended in 50 μl of buffer 10 mM Tris-HCl, pH 7.4, 0.5 mM MgCl₂, 1 mM DTT, 0.1 mM PMSF, and 250 μM GTP γS , incubated on ice for 30 min, and centrifuged. The supernatant was analyzed for the presence of G-protein subunits by immunoblotting. Results were quantified with Image Gauge (FujiFilm). Data analysis and curve fitting was in KaleidaGraph 3.6.2.

2.4. Peptides

Peptide synthesis, purification, and mass-spectrometry were as we described before (Kisselev et al., 1994). Pure peptides were stored at -85 °C, lyophilized and under nitrogen. Before the experiments the peptides were dissolved in water to obtain stock solutions of 1–10 mM, and the pH was adjusted to 7.5 with NaOH. Amino acid sequences for the peptides were as follows: Gt α CT—Gt α (340–350) (IKENLKDCGLF), Gt γ CT—Gt γ (50–71) farnesyl (EDPLVKGIPEDKNPFKELKGGC-farnesyl), which is functionally equivalent to Gt γ (60–71)farnesyl but gives more complete Meta II stabilization.

2.5. UV/visible spectroscopy

The amount of extra Meta II was measured on a Cary-50 UV/visible spectrophotometer (Varian, CA), at 4 °C, cuvette path-length 10 mm,

essentially as we described before (Kisselev et al., 1994; Kisselev et al., 1999a). Samples contained 2.5 μM of urea-washed ROS membranes, or an equal amount of the rhodopsin membranes treated with NEM and/or IAS in buffer MII (20 mM Tris-HCl, pH 8.0, 130 mM NaCl, 1 mM MgCl_2 , and 1 mM EDTA) and 2 mM of corresponding G-protein peptides. 700–250 nm spectra were recorded before and after activation of the sample with a 390 ± 5 nm light. The amount of Meta II was calculated as the absorbance difference A380–A417 before and after photoactivation. The amount of Meta II without transducin peptides added was taken as zero. Control Meta II experiments were at pH 5.5 in 80 mM 2-[N-Morpholino]-ethanesulfonic acid, MES, pH 5.5, 130 mM NaCl, 1 mM MgCl_2 , and 1 mM EDTA. Single wavelength experiments were as above, except that they utilized Cary-50's rapid scanning mode at 80 data points/s. Buffered hydroxylamine was added to the cuvette to the final concentration of 50 mM in the dark (Hofmann, Emeis, & Schnetkamp, 1983; Sakmar, Franke, & Khorana, 1991). The data were collected at 365, 405, and 500 nm in separate experiments. The total length of each scan was 10 min. No noticeable bleaching of the sample was detected due to the Cary-50 scanning beam either with or without hydroxylamine. The sample was activated halfway through the scan with a shutter-controlled Fiber-Light PL-900 equipped with a 390 ± 5 nm pass filter. The data were processed off-line using KaleidaGraph 3.6.2. Full spectra scans were normalized to zero at 700 nm. Single wavelength scans were normalized to zero using baseline absorbance values immediately before light activation. For the analysis of rates of Meta II decay, the traces were normalized to the peak maximum of Meta II.

3. Results

3.1. Chemo-selective thioalkylation of rhodopsin

We used selective thioalkylation of dark-adapted rhodopsin in native urea-washed rod outer segment membranes in order to introduce potential steric hindrances for interactions between R^* and binding domains $\text{Gt}\alpha\text{CT}$ and $\text{Gt}\gamma\text{CT}$. We used a rhodopsin modification procedure originally described by Wu and Stryer (Wu & Stryer, 1972) and by De Grip (De Grip et al., 1975), which takes advantage of the ability of *N*-ethyl-maleimide (NEM) to modify preferentially two surface cysteine residues under mild reaction conditions in the dark, while treatment with another agent, iodoacetamidosalicylate (IAS), leads to the selective modification of a single residue. After the discovery of the full amino acid sequence of bovine rhodopsin (Hargrave et al., 1983; Ovchinnikov et al., 1982), these cysteine residues have been identified as Cys 140 and Cys 316 at the cytoplasmic surface of rhodopsin, Fig. 1. Using [^3H]NEM we confirmed the reported chemo-selectivity of NEM and IAS by monitoring the incorporation of [^3H]NEM into rhodopsin with and without pre-treatment with IAS (Methods). Based on this procedure, three samples were prepared: (1) R-IAS, IAS-treated rhodopsin with Cys 316 modified, (2) R-NEM, NEM-treated rhodopsin with both Cys 140 and Cys 316 modified, and (3) R-IAS/NEM, rhodopsin treated with IAS to modify Cys 316, and then treated with NEM to modify remaining Cys 140.

3.2. Photoactivation of the modified rhodopsin

First, we studied whether the chemo-selective thioalkylation of rhodopsin would affect Meta II formation under

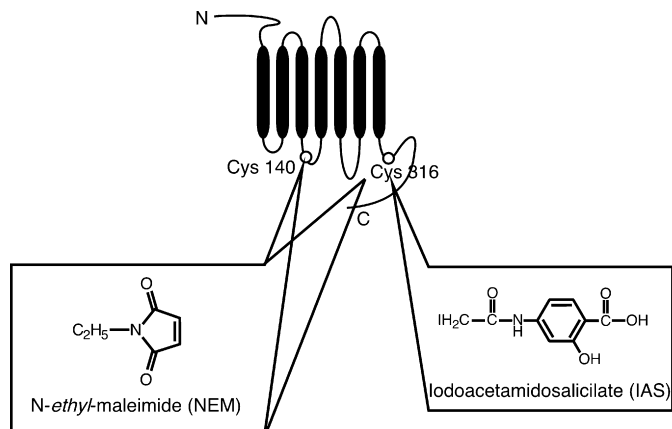


Fig. 1. A schematic presentation of two sites of chemo-selective thioalkylation of rhodopsin.

low pH conditions where Meta II is a predominant spectral intermediate. All three modified samples were indistinguishable from native rhodopsin in full dark–light UV/visible scans, Fig. 2. This experiment confirms a previous report (Resek, Farahbakhsh, Hubbell, & Khorana, 1993) that mild thioalkylation at Cys 140 and Cys 316 at the rhodopsin's cytoplasmic surface does not interfere with Meta II formation.

3.3. Stabilization of extra-Meta II

Under more basic pH 8.0, light activation of rhodopsin produces Meta I–Meta II equilibrium that is significantly shifted towards Meta I. Addition of synthetic peptides that represent $\text{Gt}\alpha\text{CT}$ and $\text{Gt}\gamma\text{CT}$ leads to extra-Meta II in a

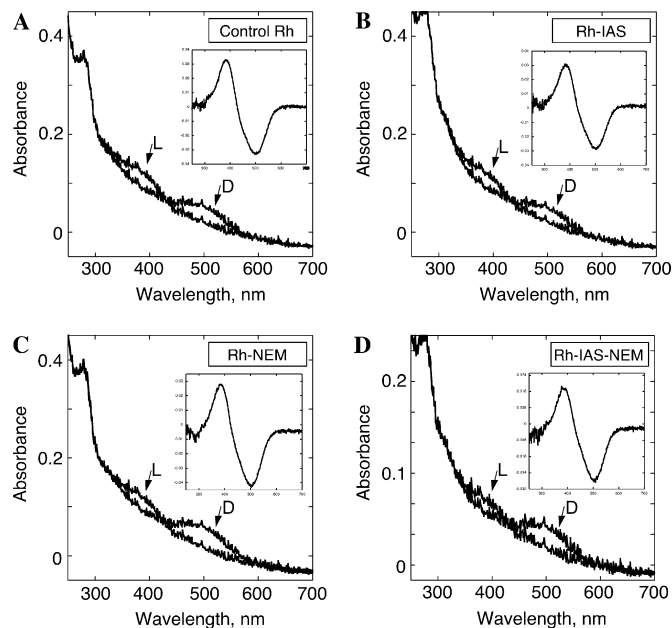


Fig. 2. UV/visible spectra of urea-washed ROS membranes. The light minus dark difference spectra are shown in insets. (A) The native rhodopsin. (B) Rhodopsin modified with IAS at Cys 316. (C) Rhodopsin modified with NEM at Cys 140 and Cys 316. (D) Double modification with IAS at Cys 316 and subsequently with NEM at Cys 140.

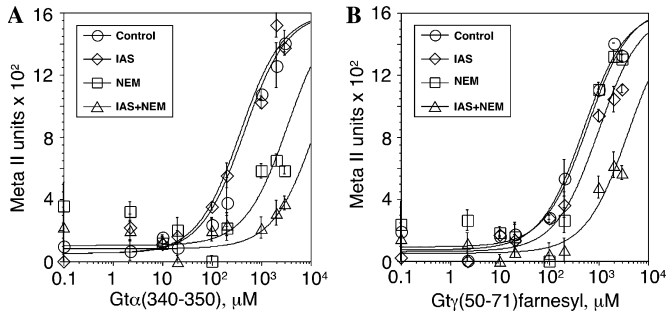


Fig. 3. Stabilization of extra Meta II by Gt α CT, Gt α (340–350) (A), and Gt γ CT, Gt γ (50–71)farnesyl (B). The type of the thioalkylating agent used for rhodopsin modification is shown with different symbols. Error bars represent standard deviation calculated from at least three independent experiments.

dose-dependent manner, an effect that mimics holo-Gt. We used this spectroscopic assay to measure whether selective modifications of Cys 140 and Cys 316 in rhodopsin would interfere with extra-Meta II signal. R-IAS showed dose-dependent Meta II formation in the presence of Gt α CT indistinguishable from native R, with $EC_{50} = 300 \mu\text{M}$. In striking contrast, R-NEM and R-IAS-NEM were unable to interact with Gt α CT effectively, showing at least a 10-fold reduction in affinity, $EC_{50} = 3 \text{ mM}$ and $EC_{50} > 10 \text{ mM}$ correspondingly, Fig. 3A. Because all rhodopsin samples showed normal dark spectra and normal Meta II formation at pH 5.5, the loss of extra-Meta II formation was not due to the partial inactivation of rhodopsin by NEM, or IAS and NEM.

Extra-Meta II measurements utilizing Gt γ CT produced a distinctly different pattern of interaction. Contrary to the lack of effect on Gt α CT binding, modifications of rhodopsin with IAS produced a 3-fold decrease in Gt γ CT affinity for R*, Fig. 3B. NEM had no effect on Meta II stabilization by Gt γ CT, while double modification, Cys 316 with IAS and subsequent modification of Cys 140 with NEM increased EC_{50} to 4 mM. Similar extra-Meta II data were obtained when pyrrolidine–nitroxide-based spin labeling reagents (IA)-PROXYL were used instead of IAS, and (MTS)-PROXYL and 3-maleimido-PROXYL were used instead of NEM. Thus, modifications of rhodopsin's Cys 140 and Cys 316 had an almost opposite effect on the ability of Gt α CT and Gt γ CT to interact with Meta II. The same rhodopsin sample modified by NEM interacted with Gt γ CT normally, but with Gt α CT poorly. Rhodopsin modified by IAS, in contrast, interacted with Gt α CT well, while Gt γ CT binding to Meta II was reduced.

3.4. Interactions with Gt

To study how the chemo-selective thioalkylation of rhodopsin would affect light-dependent binding of holo-Gt to R, R-IAS, R-NEM, and R-IAS-NEM, we independently reconstituted these rhodopsin samples with increasing amounts of Gt made from purified Gt α and Gt $\beta\gamma$. Only GDP retained on Gt α after Gt purification

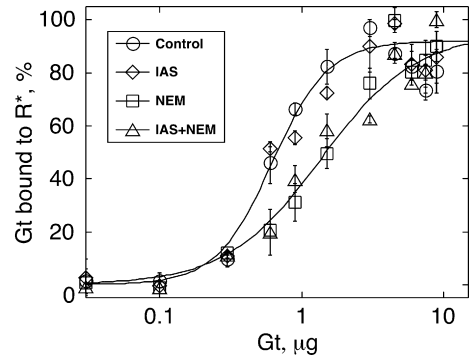


Fig. 4. Dose-dependent interaction of Gt with urea-washed ROS membranes. The type of the thioalkylating agent used for rhodopsin modification is shown with different symbols. Error bars represent standard deviation calculated from four independent experiments.

was present in the assay. The rhodopsin membranes were illuminated, washed, and then the bound Gt was examined in GTP γ S eluates by quantitative immuno-blotting, Fig. 4. Gt binding to native membranes exhibited clear signs of positive cooperative interaction, also reported earlier by Willardson (Willardson et al., 1993). Fitting the Gt binding data to the Hill equation revealed Hill coefficient 2.2 for R*–Gt interaction. When Cys 316 of rhodopsin was modified by IAS, we observed no change in the binding characteristics of Gt. When both Cys 140 and Cys 316 were modified by NEM, or IAS and NEM combination, the total level of Gt binding at high Gt concentrations did not change, which is consistent with a previous report (Reichert & Hofmann, 1984), but Gt binding lost positive cooperativity, Hill coefficient is 1.3.

3.5. Meta II decay induced by hydroxylamine

In the second set of experiments we directly examined the conformational status of Meta II produced by Gt α CT or Gt γ CT in the presence of hydroxylamine. Just as described above, after illumination under pH 8.0 and 4 °C, Meta I, $A_{\text{max}} = 478 \text{ nm}$, is the predominant photoproduct, while in the presence of synthetic peptides Gt α CT and Gt γ CT, Meta II predominates, $A_{\text{max}} = 380 \text{ nm}$, Fig. 5A and B. In the presence of 50 mM hydroxylamine dark rhodopsin is very stable. Addition of Gt α CT or Gt γ CT at 2 mM did not change dark rhodopsin stability in the presence hydroxylamine, as monitored by the absorbance change at 500 nm, showing that peptides did not influence the Schiff base accessibility, Fig. 5C. Only after light activation can hydroxylamine attack the Schiff base to form retinal oxime, $A_{\text{max}} = 365 \text{ nm}$, Fig. 5B (L + HA) (Hofmann et al., 1983; Sakmar et al., 1991). We monitored the rate of the hydroxylamine induced Meta II decay, when Meta II was produced by Gt α CT or Gt γ CT. Because of the spectral overlap between Meta II and retinal oxime peaks, Fig. 5B, we measured Meta II decay using rapid scanning spectroscopy at 405 nm. Under these conditions, light activation of the sample leads to the fast and transient formation of Meta II, which is then converted to the retinal oxime by the present

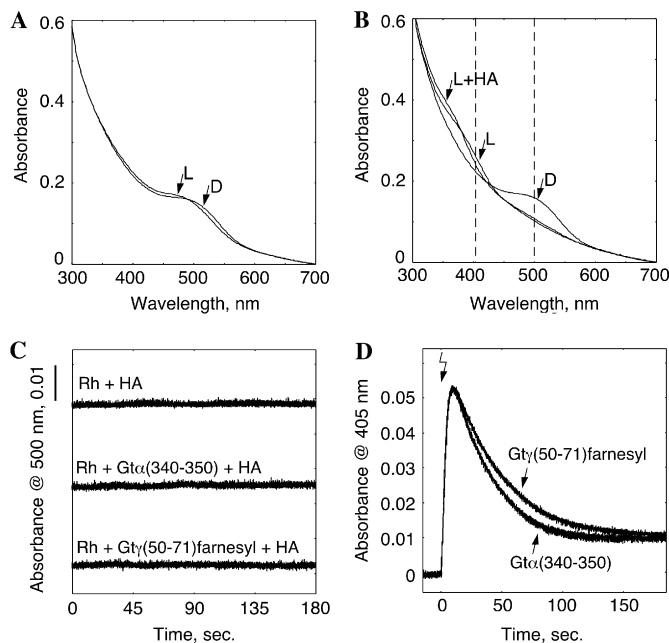


Fig. 5. Reactivity of Meta II–Gt α CT and Meta II–Gt γ CT to hydroxylamine. (A) Control UV/visible spectra of rhodopsin membranes at pH 8.0. (B) Representative UV/visible spectra of rhodopsin membranes in the presence of Gt α CT in the dark (D), after light activation (L), and after subsequent addition of hydroxylamine (L + HA). Dotted lines show wavelengths used to collect time resolved data at 500 and 405 nm. (C) Time resolved spectra of dark rhodopsin in the presence of hydroxylamine at 500 nm (Rh + HA), and after addition of Gt α CT, Gt α (340–350) (Rh + Gt α (340–350) + HA), and Gt γ CT, Gt γ (50–71)farnesyl (Rh + Gt γ (50–71)farnesyl + HA). (D) Transient formation of Meta II and hydroxylamine-induced decay. The arrow indicates the start of light activation.

hydroxylamine, Fig. 5D. The initial rate and time to peak of Meta II production were identical for both Gt α CT and Gt γ CT. Comparison of the rates of Meta II decay revealed that Meta II–Gt γ CT decays substantially slower than Meta II–Gt α CT. The rate of Meta II–Gt α CT decay was identical to the rate of Meta II decay without the peptides. We proceeded to measure how specific the effect of Gt γ CT was. The unfarnesylated Gt γ CT with identical amino acid sequence does not interact with Meta II (Kisselev et al., 1994). This control peptide produced the profile of rhodopsin bleaching in the presence of hydroxylamine indistinguishable from that of Meta II or Meta II–Gt α CT (data not shown). Thus, specific complex Meta II–Gt γ CT reacts with hydroxylamine slower than Meta II–Gt α CT.

4. Discussion

Rhodopsin-catalyzed nucleotide exchange on Gt is a complex multi-step reaction that involves several intermediate steps (Chabre & le Maire, 2005; Okada et al., 2001; Park et al., 2004; Ridge et al., 2003; Sakmar et al., 2002), multiple rhodopsin intermediates (Arnis & Hofmann, 1993; Morizumi, Imai, & Shichida, 2005) and specific domains on all subunits of Gt (Gautam et al., 1998; Hamm, 2001). Several models exist to explain the mechanism of R^{*}-catalyzed

G-protein activation. The lever-arm model (Iiri, Farfel, & Bourne, 1998) and the gear-shift model (Cherfils & Chabre, 2003) assume interactions of Gt with R^{*} monomer, and share the description of the first step, the initial docking of Gt to R^{*}, but differ in explaining the mechanism of the nucleotide release on Gt α . In short, the activating signal from R^{*} is proposed to propagate via well-defined sites on Gt α , such as the N-terminal helix, the C-terminal domain, the α 5-helix, and also via the C-terminal domain of Gt γ , shown by arrows 1 and 2 on Fig. 6. The end-result is the pulling motion by Gt $\beta\gamma$ on the Switch II region of Gt α and release of GDP. This view has originally been proposed by Bourne and is based on the analysis showing that Gt $\beta\gamma$ occupies the space of a nucleotide exchange factor for the Gt α -subunit, similar to the position of a nucleotide exchange factor EF-Ts, crystallized in complex with the nucleotide-empty elongation factor Tu (Ef-Tu) (Wang, Jiang, Meyering-Voss, Sprinzl, & Sigler, 1997). The gear-shift model incorporates this step as the engagement of the second gear, potentially necessary for the stabilization of the transient nucleotide-empty state, but it does not believe that this step is responsible for the nucleotide exchange. The gear-shift model proposes the engagement of the third gear, the third route, shown by arrow 3 on Fig. 6, and argues that a pushing motion by the N-terminal domain of Gt γ partially displaces the helical domain of Gt and triggers GDP release.

A conceptually different model of interactions between Gt and rhodopsin dimer has been proposed recently by

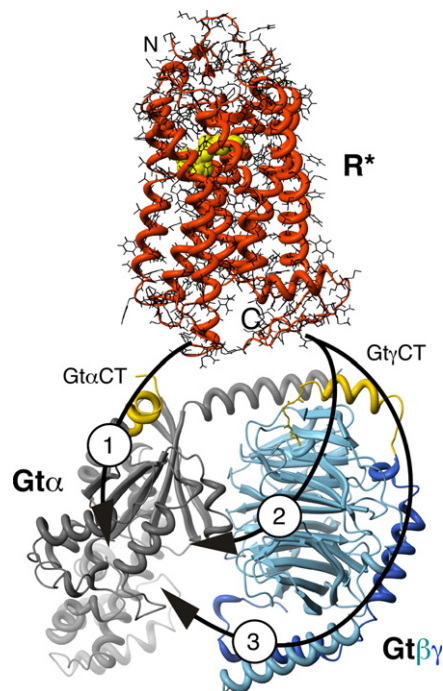


Fig. 6. Three-dimensional structures of rhodopsin (orange) and the G-protein, transducin (grey—Gt α , blue—Gt $\beta\gamma$). Rhodopsin interacting domains of Gt at the C-terminal regions of Gt α and Gt γ are shown in yellow in their R^{*}-bound conformations (Kisselev & Downs, 2003; Kisselev et al., 1998). Arrows indicate proposed mechanisms of signal propagation from R^{*} to the nucleotide-binding site of Gt α .

Palczewski (Filipek et al., 2004; Palczewski, 2006; Park et al., 2004), based on the original observation of rhodopsin dimers in the native disk membranes (Fotiadis et al., 2003). The most important feature of this model is the almost perfect match in size between RR and Gt, which explains the paradox between the large footprint on all three subunits of Gt from a relatively compact intracellular surface of R*.

In analyzing the contributions by Gt α and Gt $\beta\gamma$ into the first step of these models, we have previously proposed a two-step sequential fit model of R*–Gt interactions to explain the mechanism of signal transfer from Meta II to Gt via the C-terminal domains of Gt α (Gt α CT) and Gt γ (Gt γ CT) (Herrmann et al., 2004; Kisselev et al., 1999a). The model is based on the observation that both Gt α CT and Gt γ CT mimic holo-Gt in the ability to interact with and stabilize Meta II, but they play different roles in the activation process (Herrmann et al., 2004; Kisselev et al., 1999a). The differences can potentially be explained by interactions with multiple iso-spectral forms of Meta II, or structurally unique complementary binding sites on Meta II.

In this study, we show that chemo-selective modification of rhodopsin's Cys 140 leads to a more than 10-fold reduction of Gt α CT interactions with Meta II, while the modification of Cys 316 is inconsequential for Gt α CT binding. The pattern of interactions is reversed when Gt γ CT is used to stabilize Meta II. Gt γ CT tolerates the modification of Cys 140 very well, but its affinity for Meta II is reduced 3-fold when Cys 316 is modified, Fig. 3. It is important to note that the identification of Cys 316's involvement in the Gt γ CT binding in this study, gives an important clue as to the location of the site of Gt γ CT and Gt $\beta\gamma$ interactions with rhodopsin, the helix H8. This observation is consistent with a previous report showing that replacement of the amino acid sequence of H8 with the corresponding sequence from the β 2-adrenergic receptor abolishes interactions with Gt γ CT, as well as with Gt α CT (Ernst et al., 2000). Our data additionally support the models suggesting that Cys 140 is part of the binding site for Gt α CT (Arimoto, Kisselev, Makara, & Marshall, 2001; Janz & Farrens, 2004). With regard to the nature of the binding sites and their involvement in the Gt activation process, the data presented here clearly demonstrate that while the binding sites for Gt α CT and Gt γ CT partially overlap (Ernst et al., 2000; Herrmann et al., 2004), they are distinct enough to allow selective disruption of either Meta II–Gt α CT or Meta II–Gt γ CT interactions. Thus, during the activation process rhodopsin presents structurally distinct sites for the interactions with Gt α and Gt $\beta\gamma$ subunits, which argues for structural heterogeneity of Meta II species.

The two putative conformations of Meta II can exist in dynamic equilibrium, but they cannot exist at the same time, which argues strongly for the temporal separation of interactions between Meta II–Gt α CT and Meta II–Gt γ CT. Although Gt mimetic peptides have proven to be powerful tools in dissecting mechanism of signal transfer from R* to Gt, there are obvious limitations of this approach because it restricts analy-

sis to interactions of individual domains. It would be extremely interesting to extend the studies reported herein to the analysis of the domain interactions in R*–Gt complex.

The thioalkylation of Cys 140 had an interesting effect on dose-dependent Gt binding to the urea-washed ROS membranes. While the maximal level of binding was not affected, the cooperative nature of interactions was abolished, Fig. 4. One possible conclusion from this experiment is that allosteric interactions of Gt α and Gt γ with R* contribute to the positive cooperativity of binding. Exclusion of Gt α CT from interactions leads to the loss of the cooperative effect. A somewhat unexpected observation is that by preventing Gt α CT interactions with R*, binding of Gt and its nucleotide dependent release is not completely eliminated, Fig. 4. Perhaps Gt α can accommodate the loss of Gt α CT–rhodopsin interaction through the involvement of multiple domains.

To probe Meta II–Gt α CT and Meta II–Gt γ CT conformations, we used a well-known selective susceptibility of Meta II to hydroxylamine (Hofmann et al., 1983; Sakmar et al., 1991). In the dark state, the organization of rhodopsin's transmembrane helices protects the Schiff base from the attack by hydroxylamine, but after the light activation the reactivity to hydroxylamine is dramatically increased. We show that the rate of Meta II decay to retinal oxime is noticeably slower for Meta II–Gt γ CT than for Meta II–Gt α CT. Because Meta II is the dominant photoproduct under the experimental conditions, the rate difference of Meta II decay argues for the differential reactivity of the Schiff base in Meta II–Gt α CT and Meta II–Gt γ CT to hydroxylamine. These data strongly support the conclusion from the chemo-selective thioalkylation experiments above, that Meta II–Gt α CT and Meta II–Gt γ CT are structurally distinct.

In conclusion, we show that the sites of interactions for the C-terminal domains of Gt α and Gt γ subunits on Meta II are distinctly different. It is possible to affect one site but not the other by the chemo-selective thioalkylation of rhodopsin. In addition we show that the rates of hydroxylamine-induced Meta II decay are different, depending on whether the peptides from Gt α or Gt γ were used to stabilize Meta II. Together, our results argue for the conformational and structural heterogeneity of the active photointermediate Meta II, and provide strong support to the two-step sequential fit model, under which Gt α and Gt $\beta\gamma$ interact with unique signaling states of light-activated rhodopsin.

Acknowledgments

We thank Tom Sakmar for suggestions and stimulating discussion. Supported in part by Research to Prevent Blindness, American Heart Association and NIH GM63203 (O.G.K.).

References

- Arimoto, R., Kisselev, O. G., Makara, G. M., & Marshall, G. R. (2001). Rhodopsin–transducin interface: studies with conformationally constrained peptides. *Biophysical Journal*, 81(6), 3285–3293.

- Arnis, S., & Hofmann, K. P. (1993). Two different forms of metarhodopsin II: Schiff base deprotonation precedes proton uptake and signaling state. *Proceedings of the National Academy of Sciences of the United States of America*, 90(16), 7849–7853.
- Chabre, M., & le Maire, M. (2005). Monomeric G-protein-coupled receptor as a functional unit. *Biochemistry*, 44(27), 9395–9403.
- Cherfils, J., & Chabre, M. (2003). Activation of G-protein G α subunits by receptors through Galpha-Gbeta and Galpha-Ggamma interactions. *Trends in Biochemical Sciences*, 28(1), 13–17.
- De Grip, W. J., Bonting, S. L., & Daemen, F. J. (1975). Biochemical aspects of the visual process. Classification of sulfhydryl groups in rhodopsin and other photoreceptor membrane proteins. *Biochimica Biophysica Acta*, 396(1), 104–115.
- Ernst, O., Meyer, C., Marin, E., Henklein, P., Fu, W., Sakmar, T., & Hofmann, K. (2000). Mutation of the fourth cytoplasmic loop of rhodopsin affects binding of transducin and peptides derived from the carboxyl-terminal sequences of transducin alpha and gamma subunits. *Journal of Biological Chemistry*, 275(3), 1937–1943.
- Filipek, S., Krzysko, K. A., Fotiadis, D., Liang, Y., Saperstein, D. A., Engel, A., & Palczewski, K. (2004). A concept for G protein activation by G protein-coupled receptor dimers: the transducin/rhodopsin interface. *Photochemical & Photobiological Sciences*, 3(6), 628–638.
- Findlay, J. B., Barclay, P. L., Brett, M., Davison, M., Pappin, D. J., & Thompson, P. (1984). The structure of mammalian rod opsins. *Vision Research*, 24(11), 1501–1508.
- Fotiadis, D., Liang, Y., Filipek, S., Saperstein, D. A., Engel, A., & Palczewski, K. (2003). Atomic-force microscopy: rhodopsin dimers in native disc membranes. *Nature*, 421(6919), 127–128.
- Gautam, N., Downes, G. B., Yan, K., & Kisselev, O. (1998). The G-protein betagamma complex. *Cellular Signalling*, 10(7), 447–455.
- Hamm, H. E. (2001). How activated receptors couple to G proteins. *Proceedings of the National Academy of Sciences of the United States of America*, 98(9), 4819–4821.
- Hamm, H. E., Deretic, D., Arendt, A., Hargrave, P. A., Koenig, B., & Hofmann, K. P. (1988). Site of G protein binding to rhodopsin mapped with synthetic peptides from the alpha subunit. *Science*, 241(4867), 832–835.
- Hargrave, P. A. (2001). Rhodopsin structure, function, and topography the Friedenwald lecture. *Investigative Ophthalmology & Visual Science*, 42(1), 3–9.
- Hargrave, P. A., McDowell, J. H., Curtis, D. R., Wang, J. K., Juszczak, E., Fong, S. L., Rao, J. K., & Argos, P. (1983). The structure of bovine rhodopsin. *Biophysics of Structure and Mechanism*, 9(4), 235–244.
- Herrmann, R., Heck, M., Henklein, P., Kleuss, C., Hofmann, K. P., & Ernst, O. P. (2004). Sequence of interactions in receptor-G protein coupling. *Journal of Biological Chemistry*, 279(23), 24283–24290.
- Hofmann, K. P., Emeis, D., & Schnetkamp, P. P. (1983). Interplay between hydroxylamine, metarhodopsin II and GTP-binding protein in bovine photoreceptor membranes. *Biochimica et Biophysica Acta*, 725(1), 60–70.
- Hong, K., & Hubbell, W. L. (1972). Preparation and properties of phospholipid bilayers containing rhodopsin. *Proceedings of the National Academy of Sciences of the United States of America*, 69(9), 2617–2621.
- Iiri, T., Farfel, Z., & Bourne, H. R. (1998). G-protein diseases furnish a model for the turn-on switch. *Nature*, 394(6688), 35–38.
- Janz, J. M., & Farrens, D. L. (2004). Rhodopsin activation exposes a key hydrophobic binding site for the transducin alpha-subunit C terminus. *Journal of Biological Chemistry*, 279(28), 29767–29773.
- Kisselev, O. G. (2005). Focus on molecules: rhodopsin. *Experimental Eye Research*, 81, 366–367.
- Kisselev, O. G., & Downs, M. A. (2003). Rhodopsin controls a conformational switch on the transducin gamma subunit. *Structure (Camb)*, 11(4), 367–373.
- Kisselev, O. G., Ermolaeva, M. V., & Gautam, N. (1994). A farnesylated domain in the G protein gamma subunit is a specific determinant of receptor coupling. *Journal of Biological Chemistry*, 269(34), 21399–21402.
- Kisselev, O. G., Kao, J., Ponder, J. W., Fann, Y. C., Gautam, N., & Marshall, G. R. (1998). Light-activated rhodopsin induces structural binding motif in G protein alpha subunit. *Proceedings of the National Academy of Sciences of the United States of America*, 95, 4270–4275.
- Kisselev, O. G., Meyer, C. K., Heck, M., Ernst, O. P., & Hofmann, K. P. (1999a). Signal transfer from rhodopsin to the G-protein: Evidence for a two-site sequential fit mechanism. *Proceedings of the National Academy of Sciences of the United States of America*, 96, 4898–4903.
- Kisselev, O. G., Pronin, A. P., & Gautam, N. (1999b). Transient Expression of the beta/gamma-complex in fibroblasts and reconstitution assays with a receptor, rhodopsin. In D. R. Manning (Ed.), *G-proteins: Techniques of Analysis* (pp. 85–95). CRC Press.
- Morizumi, T., Imai, H., & Shichida, Y. (2005). Direct observation of the complex formation of GDP-bound transducin with the rhodopsin intermediate having a visible absorption maximum in rod outer segment membranes. *Biochemistry*, 44(29), 9936–9943.
- Okada, T., Ernst, O. P., Palczewski, K., & Hofmann, K. P. (2001). Activation of rhodopsin: new insights from structural and biochemical studies. *Trends in Biochemical Sciences*, 26(5), 318–324.
- Ovchinnikov, I. A., Abdulaev, N. G., Feigina, M., Artamonov, I. D., Zolotarev, A. S., Kostina, M. B., Bogachuk, A. S., Moroshnikov, A. I., Martinov, V. I., & Kudelin, A. B. (1982). The complete amino acid sequence of visual rhodopsin. *Biorganicheskaya Khimiya*, 8, 1011–1014.
- Palczewski, K. (2006). G protein-coupled receptor rhodopsin. *Annual Review of Biochemistry*, 75, 743–767.
- Papermaster, D. S., & Dreyer, W. J. (1974). Rhodopsin content in the outer segment membranes of bovine and frog retinal rods. *Biochemistry*, 13(11), 2438–2444.
- Park, P. S., Filipek, S., Wells, J. W., & Palczewski, K. (2004). Oligomerization of G protein-coupled receptors: past, present, and future. *Biochemistry*, 43(50), 15643–15656.
- Reichert, J., & Hofmann, K. P. (1984). Sulfhydryl group modification of photoreceptor G-protein prevents its light-induced binding to rhodopsin. *FEBS Letters*, 168(1), 121–124.
- Resek, J. F., Farahbakhsh, Z. T., Hubbell, W. L., & Khorana, H. G. (1993). Formation of the meta II photointermediate is accompanied by conformational changes in the cytoplasmic surface of rhodopsin. *Biochemistry*, 32(45), 12025–12032.
- Ridge, K. D., Abdulaev, N. G., Sousa, M., & Palczewski, K. (2003). Phototransduction: crystal clear. *Trends in Biochemical Sciences*, 28(9), 479–487.
- Sakmar, T. P., Franke, R. R., & Khorana, H. G. (1991). The role of the retinylidene Schiff base counterion in rhodopsin in determining wavelength absorbance and Schiff base pKa. *Proceedings of the National Academy of Sciences of the United States of America*, 88(8), 3079–3083.
- Sakmar, T. P., Menon, S. T., Marin, E. P., & Awad, E. S. (2002). Rhodopsin: insights from recent structural studies. *Annual Review of Biophysics and Biomolecular Structure*, 31, 443–484.
- Sale, G. J., Towner, P., & Akhtar, M. (1977). Functional rhodopsin complex consisting of three noncovalently linked fragments. *Biochemistry*, 16(25), 5641–5649.
- Wang, Y., Jiang, Y., Meyering-Voss, M., Sprinzl, M., & Sigler, P. B. (1997). Crystal structure of the EF-Tu.EF-Ts complex from *Thermus thermophilus*. *Nature Structural Biology*, 4(8), 650–656.
- Willardson, B. M., Pou, B., Yoshida, T., & Bitensky, M. W. (1993). Cooperative binding of the retinal rod G-protein, transducin, to light-activated rhodopsin. *Journal of Biological Chemistry*, 268(9), 6371–6382.
- Wray, W., Boulikas, T., Wray, V. P., & Hancock, R. (1981). Silver staining of proteins in polyacrylamide gels. *Analytical Biochemistry*, 118(1), 197–203.
- Wu, C. W., & Stryer, L. (1972). Proximity relationships in rhodopsin. *Proceedings of the National Academy of Sciences of the United States of America*, 69(5), 1104–1108.
- Yamazaki, A., Bartucca, F., Ting, A., & Bitensky, M. W. (1982). Reciprocal effects of an inhibitory factor on catalytic activity and noncatalytic cGMP binding sites of rod phosphodiesterase. *Proceedings of the National Academy of Sciences of the United States of America*, 79(12), 3702–3706.